Inflammatory Changes after Cryosurgery-Induced Necrosis in Human Melanoma Xenografted in Nude Mice

Silvina Gazzaniga,* Alicia Bravo,† Silvana R. Goldszmid,*‡ Fabricio Maschi,§ Julio Martinelli,† José Mordoh,‡ and Rosa Wainstok*

*Departamento de Química Biológica, Facultad de Ciencias Exactas y Naturales, Universidad de Buenos Aires, Argentina; †Hospital Eva Perón, Buenos Aires, Argentina; ‡Instituto de Investigaciones Bioquímicas, Fundación Campomar, IIB-BA (CONICET), IIB-FCEyN, Buenos Aires, Argentina; §Cátedra de Animales de Laboratorio y Bioterio, Facultad de Ciencias Veterinarias, Universidad Nacional de La Plata, Argentina

There is growing evidence that necrosis, instead of apoptosis, could act as a natural adjuvant, which could activate an immune response. In this work we have investigated if induction of tumor necrosis could trigger the affluence of inflammatory cells at the tumor site, and thus induce an immune response. For this purpose, a liquid N_2 spray was applied on human melanoma (IIB-MEL-J cell line) xenografted in nude mice and 24 h later some mice received intratumorally a single 500 U dose of recombinant murine granulocyte macrophage-colony-stimulating factor. 77–100% of the tumor mass underwent necrosis. Congestion, edema, and endothelial cell activation were the first noticeable events. A quick infiltrative response of polymorphonuclear leukocytes around the tumor was detected 24 h after liquid N_2 application, peaking at day 3. Massive macrophage recruitment was observed since day 3. An early intratumoral infiltration with inflammatory cells was only detected in the group that received recombinant murine granulocyte macrophage-colony-stimulating factor after necrosis induction by liquid N_2. Coexisting DEC 205- and F4/80-positive cells increased in number, and their localization was predominantly peritumoral after necrosis. Antibody response was only detected in the groups with tumor-induced necrosis. Our results suggest that cryosurgery-induced necrosis could be a useful model to analyze the interaction among necrosis, inflammation, and the generation of an immune response. *Key words: cryosurgery/granulocyte-monocyte colony-stimulating factor/inflammatory infiltrate/melanoma. J Invest Dermatol 116:664–671, 2001*

Whereas primary human melanoma frequently triggers a lymphoid reaction, this ability appears to be lost in metastasis, as analysis of different melanoma metastatic sites revealed scarce lymphoid infiltration (Hernberg *et al*, 1997). The reasons for this discrepancy are not known, but among several other causes, the lack of lymphocytes arrival into tumors could be due to an abortion of the immune response at the primary site by clonal deletion of reacting lymphocytes or by the release of immunosuppressive factors by tumor cells (Morvillo *et al*, 1996). Even if intratumoral lymphocytes are present, another mechanism that tumor cells would employ to escape immune response would be the downregulation of major histocompatibility complex class I molecules. Along this line, when conditions for the priming of tumor-specific response were examined in mice, no detectable presentation of major histocompatibility complex class I restricted tumor antigens by the tumor itself was found (Huang *et al*, 1994). Rather, tumor antigens were exclusively cross-presented by bone marrow derived antigen-presenting cells (APC) (Bennett *et al*, 1997). Although details on the cross-priming by APC and on the underlying mechanisms that permit exogenous antigens to enter the otherwise endogenous class I presentation pathway are not fully characterized, it appears likely that the class I restricted antigens should be accessible to the cross-presenting APC, in the form of cell-associated debris or particulate in nature (Bennet *et al*, 1997).

The final consequence of the interplay of these and other factors is that the spontaneous immune response to progressing melanoma is inefficient. Our interest is to develop an efficient immune response. It is accepted that apoptosis, as a normal physiologic mechanism, proceeds without inflammation and would thus be unable to generate an immune response. There is growing evidence, instead, that necrosis could act as a natural adjuvant, which could activate APC and initiate an immune response (Gallucci *et al*, 1999).

Cryosurgery is a well-aimed and controlled procedure to induce tissular necrosis by the application of liquid N_2, and it was chosen as it is rapid, efficient and the results could eventually be reproduced in a clinical setting (Zouboulis, 1999). The biologic changes that occur during and after cryosurgery have been studied *in vitro* and *in vivo* (Orpwood, 1981; Mazur, 1984). Tissue injury is induced by cell freezing and by the vascular stasis developed after thawing. Therefore, the cryoreaction is characterized by physical and vascular phases. A postulated third immunologic phase has not been fully studied for malignant skin lesions (Zouboulis, 1999).

In order to study in the first place the innate immune response, which recent experiments point as essential in the development of

Manuscript received January 21, 2000; revised November 7, 2000; accepted for publication January 19, 2001.

Reprint requests to: Dr. Rosa Wainstok, Dpto. Química Biológica, 4 Piso, Pabellón II, Ciudad Universitaria (1428) Nuñez, Buenos Aires, Argentina. Email: rwains@qb.fcen.uba.ar

Abbreviations: rmGM-CSF, recombinant murine granulocyte macrophage-colony-stimulating factor; HPF, high power field; APC, antigen-presenting cell; DC, dendritic cells.

an effective immune response (Clynes *et al*, 1998), we have investigated if the rapid induction of necrosis in experimental melanoma could trigger the affluence of inflammatory cells to the tumor site and the induction of anti-tumoral antibody formation. We also performed an exploratory approach to analyze if intratumoral injection of recombinant murine granulocyte macrophage-colony-stimulating factor (rmGM-CSF) after cryosurgery could enhance the affluence of dendritic cells (DC), which may process necrotic cells and released antigens.

GM-CSF is a 24 kDa glycosylated cytokine (Burges *et al*, 1977) that plays a vital part in various functions of the immune system. Among its key activities, GM-CSF enhances macrophage cytotoxicity (Wing *et al*, 1989) and DC maturation (Szabolcs *et al*, 1996) and migration (Shutt *et al*, 2000). These properties, found *in vitro,* may constitute the basis for the beneficial effect of GM-CSF when different clinical and experimental approaches were studied. Intralesional application of GM-CSF (Si *et al*, 1996), intradermal administration of the cytokine for stage IV melanoma patients (Nasi *et al*, 1999), GM-CSF-secreting tumor cells vaccines (Dranoff *et al*, 1993; Soiffer *et al*, 1998) or DC transduced with GM-CSF-expressing viral vectors (Klein *et al*, 2000) have demonstrated improved anti-tumoral responses.

MATERIALS AND METHODS

Cell lines MCF-7 (human adenocarcinoma) (Soule *et al*, 1973); B16-F1 (murine melanoma) kindly provided by Dr A. Vecchi, Milan, Italy; 1G11 (murine microvascular endothelium) (Dong *et al*, 1997); IIB-MEL-J (Guerra *et al*, 1989); IIB-MEL-IAN and IIB-MEL-LES (Kairiyama *et al*, 1995) (human melanoma) cell lines were employed. Every cell line was cultured according to the indications reported in the original publications, and they were all tested to be mycoplasm free. IIB-MEL-J was also grown subcutaneously in nude mice (IIB-MEL-J_{nude}) and maintained by *in vivo* passages.

Animals Athymic male NIH (S)-nu, 6–8 wk old, were obtained from the Faculty of Veterinary Sciences Facility (University of La Plata, Buenos Aires).

Tumors To produce IIB-MEL-J tumors, approximately 1 mm^3 tumor fragments were subcutaneously implanted by trocar in the left leg. Animals were controlled weekly until tumors were visually detected. Mice were treated when the tumors measured less than 10 mm in their largest dimension. Animals were randomly assigned to control and treatment groups (n = 3–4 animals per group per experiment). At least three experiments were performed.

For evaluation of tumor growth, measures were taken with caliper before treatment and on being killed. Tumor sizes are expressed following the formula $(A \times B^2)/2$, where A is the largest and B is the shortest dimension.

Treatment groups Groups treated with cryosurgery: animals were anesthetized with an intraperitoneal injection of 0.3 ml of 5 mg per ml sodium pentobarbital. An intermittent liquid N_2 spray (Cry-A-C device, Brymill, Ellington, CT) was applied by an experienced dermatologist (JMa) on the skin over the tumor during a time adjusted to tumor size. The maximum application time to the larger tumors was 45 s. The spray was emitted from a distance of 1–2 cm from the target at a 90° angle. A needle thermocouple was placed with its tip at the periphery of the tumor to evaluate the temperature reached during freezing. After the procedure, mice were kept on a heating pad until they recovered from anesthesia. This point in treatment was taken as day 0. One day later, one group of mice received a single dose of 500 U rmGM-CSF (EC_{50}: 0.12 ng per ml) (Sigma, St Louis, MO) applied intratumorally with a $27\frac{1}{2}$ G needle tuberculin syringe (Terumo Medical Corporation, Elkton, MD).

Control groups All the animals were anesthetized. A group of tumor-bearing mice remained untreated. For the group only receiving rmGM-CSF, one intratumoral dose was applied as described above. To evaluate the effect of the intratumoral injection itself or in conjunction with necrosis, one group of tumor-bearing mice were injected with phosphate-buffered saline (PBS) –0.1% bovine serum albumin (BSA; vehicle used for rmGM-CSF reconstitution). In another group, animals were cryotreated previous to vehicle injection. Animals from all groups were killed on days 3 or 15.

Tissue and sera processing Before being killed, blood was drawn by cardiac puncture from anesthetized mice. After clotting and centrifugation, sera were fractionated and stored at –80°C. For every group, tumors were bisected: one-half of each specimen was fixed in 10% buffered formalin, embedded in paraffin, sectioned at 4–7 μm and stained with hematoxylin–eosin. The other half was frozen and stored at –80°C for immunohistochemistry. Briefly, cryostat sections were acetone-fixed, blocked with 5% normal rabbit serum and incubated with optimal dilutions of the primary monoclonal antibodies (MoAb). Rat anti-mouse MoAb used were RB6–5CG (Pharmingen, San Diego, CA) for polymorphonuclear leukocytes (PMN), F4/80 (Serotec Ltd, U.K.) for macrophages, TMβ-1 and DEC 205 (hybridoma supernatant, kindly provided by Dr A. Vecchi, Istituto Mario Negri, Milan, Italy) for natural killer cells and DC, respectively. The specific binding was revealed using 1/100 goat anti-rat IgG (Sigma), 1/500 rat peroxidase/anti-peroxidase complex (Accurate Chemicals) and 0.05% 3,3′-diaminobenzidine (Sigma) plus 0.03% H_2O_2. Endogenous peroxidase activity was blocked with 0.3% H_2O_2.

Humoral response This was determined by enzyme-linked immunosorbent assay and immunofluorescence. Enzyme-linked immunosorbent assay was performed as previously described (Capurro *et al*, 1998). Briefly, 10^4 exponentially growing IIB-MEL-J cells were plated in 96-well plates and left overnight for adherence. They were then washed twice with PBS, fixed for 10 min with 4% buffered formalin and washed again three times with PBS. The wells were blocked with PBS–1% BSA for 1 h, after which 1/25 and 1/50 dilutions of mice sera were incubated overnight at 4°C. After washing three times with PBS–0.1% BSA, a peroxidase-conjugated rabbit anti-total mouse immunoglobulin (Dako Corporation, CA) 1/250 was added for 90 min. After washing several times with PBS–0.1% BSA, the reaction was developed with o-phenylenediamine and read at 415 nm.

The immunofluorescence assay was performed as described (Ballaré *et al*, 1995). Briefly, 4% formalin-fixed cells were blocked with 10% normal goat serum. Mice sera were used as above and specific binding was detected with fluorescein isothiocyanate goat anti-mouse antibody (Sigma).

Quantitative evaluations Determinations were performed with an image analyzer (KS 300 Kontron Electronik) coupled to an Axioplan microscope (Zeiss, Germany). The distance (in μm) between the basal membrane of the epidermis and the tumor border was measured in 10 fields per sample at ×25 magnification. Total tumor and necrotic areas were evaluated under the same conditions. PMN and macrophages were counted in at least 10 fields per sample at ×1000 magnification (high-power field, HPF).

Statistical analysis Data on infiltrating cells (PMN and macrophages) were established by computing medians and ranks for each group examined. Tests for differences between pretreatment and post-treatment levels were calculated using the nonparametric Wilcoxon rank test. Data on tumor growth, edema, and necrosis were statistically analyzed using the Student's t test (two-tailed).

RESULTS

Sequential morphologic analysis The time course of the reaction to freezing in tumor-bearing mice after cryosurgery was initially analyzed in order to determine the presence and nature of inflammatory cells and other noncellular accompanying events. The results are summarized in **Table I**. Congestion, edema, and endothelial cells activation were the first noticeable events, as early as 1.5 h after liquid N_2 spray. At this time an early response of PMN leukocytes, which were densely recruited intravascularly with scarce or null extravasation was also noticed. Later on, PMN massively infiltrated the peritumoral area and reached their maximal concentration at day 3. At day 15, these cells had notoriously decreased. Macrophages were scarcely observed 24 h postliquid N_2 application, became more abundant at day 3 and peaked at day 7, persisting until the end of the observation period. The histologic identities of these cells were confirmed immunohistochemically with MoAb RB6-5CG for PMN (not shown) and MoAb F4/80 for macrophages (**Fig 1*A*, *B***).

Both intratumoral and peripheral vascular endothelium were also affected. Hyperplastic, swelling cells with epithelioid appearance were early morphologic evidences of endothelium activation. Fifteen days later, intratumoral endothelium (**Table I**) reversed to a

Table I. Time course of some morphologic changes postcryosurgery[a]

Time post-treatment	Macrophages	PMN	Tumor necrosis	Fibroblasts	Congestion	Edema	Collagen	Activated EC[d]
Day –1 (untreated)	–	–	–	+	no	no	Unmodified	no
1.5 h	±	± +++[b]	±[c]	+	+++	++++	Unmodified	+
6.5 h	±	+++	±[c]	+	+++	++++	Unmodified	+
Day 1	+	+++	±[c]	+	+++	++++	Unmodified	+
Day 3	+++	++++	++++	+	+++	+++	Unmodified	++
Day 7	++++	++	++++	++	+++	++	++	++
Day 15	+++	+	++	+++	no	+	++++	+

[a]Data correspond to semiquantitative evaluations in the periphery of the tumor on hematoxylin–eosin sections. Two independent experiments were performed in triplicate.
[b]Cells observed in the lumen of vessels.
[c]Tumor cells depicting initial evidence of necrosis.
[d]EC, endothelial cells.

less activated phenotype displaying plane morphology. In untreated tumor samples, only plane endothelial cells were observed. Early vascular damage could be assumed by the presence of erythrocyte extravasation until day 3 post-treatment.

Accompanying these cellular events, a rapid edema (1.5 h) (**Table I**) was recorded that slowly decreased from day 7 until the end of the observation period. Stromal peritumoral fibroblasts showed an inverse kinetics, increasing in size and number from days 7 to 15. Collagen accumulation was a late phenomenon. Considering these observations, days 3 and 15 were selected to analyze the infiltrative phenomenon in more detail and to evaluate the effect of rmGM-CSF.

Treatment groups The characteristics of the treatments received by different groups are listed in **Table II**. rmGM-CSF was injected intratumorally, as the main objective was to investigate if DC could enter the necrotic mass and thus enhance the immune response.

Tumor growth, necrosis, and edema Whereas tumors from groups I, III, and V continued growth between days 3 and 15 (**Fig 2**), tumor progression was arrested in groups subjected to cryosurgery (II, IV, and VI); however, in these groups, complete regression was only observed in six of 20 mice, in which tumor tissue was completely replaced by necrotic masses and fibrosis.

As it refers to necrosis from group I, histologic examination at day 3 revealed viable tumor cells, a well defined boundary between tumor and dermis and absence of edema (**Fig 3*A***). Examination of tumors from groups II and IV at day 3 showed significant necrosis of the tumor mass, ranging from 77 to 100% (**Figs 3*B*** and **4**). Viable tumor cells as judged by hematoxylin–eosin staining, however, were still present and their regrowth probably accounted for the diminution in percentages of necrosis at day 15 (**Fig 4**).

Edema was only detected in mice from groups II, IV, and VI (**Fig 5**). This is in accordance with an important afflux of inflammatory cells infiltrating the dermis between epidermis and tumor (**Fig 3*C***). The distance between the epidermis and tumor border in cryotreated groups remained almost unchanged at day 15 as initial edema was substituted by reparative tissue and collagen deposition (**Fig 5**).

Evaluation of the infiltrate A more detailed analysis of the infiltrate to quantitate the two predominant populations, PMN and macrophages, is presented in **Table III**.

Peritumorally, a significant increase of PMN was found in cryotreated groups with respect to controls, with up to 150 PMN per HPF. The macrophage population was also significantly recruited to the periphery of the tumor. It was possible to find almost 150 macrophages per HPF in areas of maximal influx (**Table III**). This afflux was apparently mostly due to necrosis, as neither the addition of rmGM-CSF (**Table III**, group IV) or vehicle (**Table III**, group VI) increased peritumoral PMN and macrophage accumulation. The distribution of inflammatory cells was not homogeneous in the deep dermis of groups II and IV, as even within highly infiltrated areas, denser clusters of PMN and macrophages were found.

In group III (rmGM-CSF alone), peritumoral macrophages were significantly more abundant than in the untreated tumor-bearing mice (group I), although less than in groups II and IV. A similar response to rmGM-CSF could probably be also taking place in group IV, although the high density of infiltration evoked by necrosis could be masking this effect. At the end of the observation period (day 15) the density of the peripheral infiltrate was much less than at day 3, but still significantly higher for groups II and IV.

Intratumorally (**Table III**), the infiltration of PMN and macrophages was less important than at the periphery, with less than 34 and 37 cells per HPF, respectively. In this environment, necrosis by itself does not appear to have the same potency of recruitment, as group II showed no significant difference with respect to control groups; however, although a single injection of rmGM-CSF coupled to cryosurgery had no additive effect on tumor-surrounding infiltrate, the intratumoral recruitment was significantly augmented. Both PMN and macrophages were more abundant when compared not only with controls but also to group II. At day 15, tumor cell infiltration in group IV was still significantly higher with respect to control groups. This suggests that rmGM-CSF combined to necrosis favors a lasting intratumoral infiltration.

Concerning natural killer cell infiltrates, no significant augmentation was found after 3 d. The scarce presence of natural killer cells occurred peritumorally only in some cryotreated tumors (data not shown). Cryotreated groups attained 35 natural killer cells per 100 HPF as compared with 0–7 natural killer cells per 100 HPF present in the dermis of control samples.

A comparative study between macrophages and DC was performed in tumor samples from day 3 (**Fig 1**). In tumors from group I, scarce Langerhans cells in the epidermis (not shown) and scattered macrophages and DEC205-positive cells were visualized in the dermis (**Fig 1*A***, ***C***). Similar results were obtained for tumors from group V (data not shown). In group III, injected with rmGM-CSF, the number of DEC 205-positive cells with varied morphology augmented in the basal layer of epidermis and in dermis (data not shown). Macrophages also changed their localization to peritumoral areas, consistent with data reported above in the quantitative analysis of this group. When necrosis was induced F4/80 staining pattern changed dramatically. There was not only an augmented number of positive cells (**Fig 1*B***), but also an increased intensity of staining. DEC 205-positive cells (putative DC) were

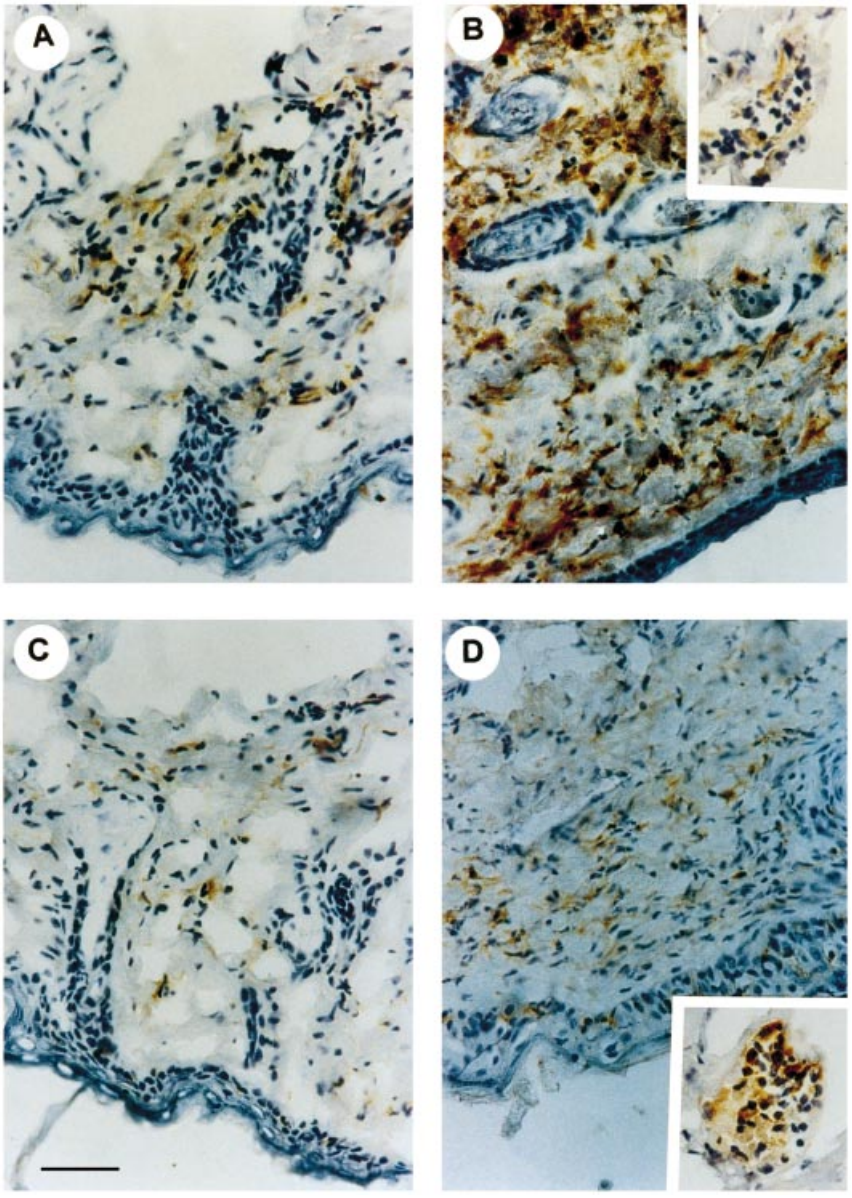

Figure 1. Comparative analysis of macrophages and DC populations 3 d post-treatment. (A) Immunohistochemical detection for F4/80-positive macrophages in the tumor-adjacent dermis from a group I mouse. (B) A representative area from a group IV mouse showing the peritumoral adjacent dermis densely populated with F4/80-positive cells. *Inset*: F4/80-negative inflammatory cells at the lumen of a dermic vessel. (C) Immunohistochemical staining for DEC 205-positive cells performed in consecutive sections from the same tumor depicted in (*A*). (D) an increased number of DC close to necrotic areas is observed in peritumoral dermis from a group IV mouse. *Inset*: Cells within the same vessel as in (*B*) demonstrate intense positivity for DEC 205. *Scale bar*: 2.5 μm; *insets*, 2.27 μm.

only found to increase in tumor-surrounding dermis (**Fig 1*D***). Remarkably, DEC 205-positive/F4/80-negative clusters were occasionally found within dermic venules (**Fig 1*B***, ***D***, insets).

Humoral response To determine whether cryosurgery resulted in the generation of antibodies recognizing human melanoma cells, we screened mice sera by enzyme-linked immunosorbent assay assays. Significant augmentation of reactivity with respect to untreated tumor-bearing mice was observed in eight of 20 mice from cryotreated groups II and IV. A nonsignificant level of positivity was found for groups I, III, and V (**Fig 6*A***). Serum samples from the different groups were analyzed for antibody isotypes by immunodiffusion (data not shown). Only IgM and IgG3 isotypes were detected with varying relative amounts in different animals. IgG3 augmentation was only detected in some sera from groups II and IV.

The specificity of antibodies was also tested by immunofluorescence. Mice sera from groups II and IV revealed an intense reactivity against IIB-MEL-J cells as compared with a faint positivity obtained with sera from group I (**Fig 6*B***, ***D***). Normal sera were completely nonreactive. The same intense positivity against IIB-MEL-J obtained with sera from group II was also observed against the human melanoma cell lines IIB-MEL-IAN and IIB-MEL-LES and the human mammary adenocarcinoma cell line MCF-7. Positivity was also found against human lymphocytes but not monocytes, suggesting that the antibodies developed could be partially directed against normal human antigens. Positivity

Table II. Description of experimental groups

	Animals/group		
Groups	Day 3	Day 15	Treatment
I	8	9	Untreated tumor-bearing mice
II	8	10	Cryosurgery only
III	8	10	Local rmGM-CSF
IV	8	10	Cryosurgery + local rmGM-CSF
V	8	8	Vehicle
VI	8	8	Cryosurgery + vehicle

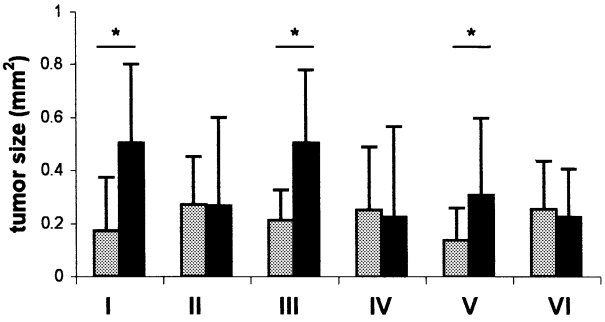

Figure 2. Tumor sizes when animals were killed. Data correspond to tumor sizes taken at day 3 (light bars) and at day 15 (dark bars) and are expressed as mean ± SEM (n = 8–10 animals per group). Treatments applied to groups I–VI are described in **Table II**. *p = 0.03 (day 3 *vs* day 15, group I), p = 0.02 (day 3 *vs* day 15, group III), and p = 0.03 (day 3 *vs* day 15, group V).

against murine cell lines was extremely weak and showed no differences among groups I, II, and IV (**Table IV**).

DISCUSSION

Rapid freezing and slow thawing is the key strategy for cell destruction by cryosurgery (Orpwood, 1981; Mazur, 1984; Turk *et al*, 1999; Zouboulis, 1999). Various cell populations present distinct abilities to tolerate cold, and melanocytes are the most sensitive skin cells to low temperatures. The consequent membrane disruption and cellular contents release could behave as attracting signals to inflammatory cells. Within hours, we observed a very rapid response of PMN to injury, with densely populated vessels but scarce extravasation. Rapid morphologic changes of endothelial cells such as hyperplasia, swelling, and nuclei protrusion to the lumen would indicate an activated state, as also reported by others (Cotran and Pober, 1988). The probable induction of selectins (Springer, 1994) would promote PMN adhesion to endothelial cells and subsequent extravasation around and within the tumor. At a later phase macrophages were also recruited, their more abundant number being attained 3 d later, and their persistence at the tumor site being longer lasting than PMN. These results diverge from those obtained by Turk *et al* (1999) after cryosurgery in a prostate cancer model, where the inflammatory infiltrate was no longer present at 72 h. It is interesting to note that the timing and some of the events evoked by cryosurgery-induced necrosis are very similar to the necrosis and inflammatory reaction generated by other treatments to human melanoma, such as limb perfusion with tumor necrosis factor-α and melphalan (Nooijen *et al*, 1998). This similarity suggests that once tumor necrosis is established, the ensuing inflammatory mechanisms could be similar.

It has recently been reported that necrotically killed cells activate endogenous signals of distress responsible for the recruitment of DC, stimuli that would not be generated by healthy or apoptotically dying cells (Gallucci *et al*, 1999). Even more, exposure of immature DC to those stimuli provides maturation signals, critical for the initiation of immunity (Sauter *et al*, 2000). Our results are consistent with this evidence because when necrosis was provoked by cryosurgery, changes in DC quantity and distribution were recorded. Migration from the epidermis to the deeper layers of the dermis would reflect an acquired ability of these cells to present antigens in their transit to the draining lymph node (Kimber *et al*, 2000).

It is also important to point out the increased macrophage population and their probable activated state, suggested by the increase in reactivity to MoAb F4/80 (see **Fig 1*B***), as consequences of cryosurgical treatment in our experimental model. This evidence does not lack relevance as not only DC may act as APC, but some inflammatory monocytes became macrophages at the subcutaneous tissue and after phagocytosis could differentiate into lymph node DC (Randolph *et al*, 1999). The concomitant existence of PMN and macrophages could be beneficial because, as it has been hypothesized (Wells and Malkovsky, 2000), when tumor cells die, the released intracellular contents, including heat shock proteins, could activate neighboring PMN to produce proinflammatory cytokines and recruit APC. Heat shock proteins complexed with tumor-derived antigenic peptides would be taken up by activated macrophages and in turn cross-presented to tumor-specific T cells via major histocompatibility complex class I (Bennett *et al*, 1997).

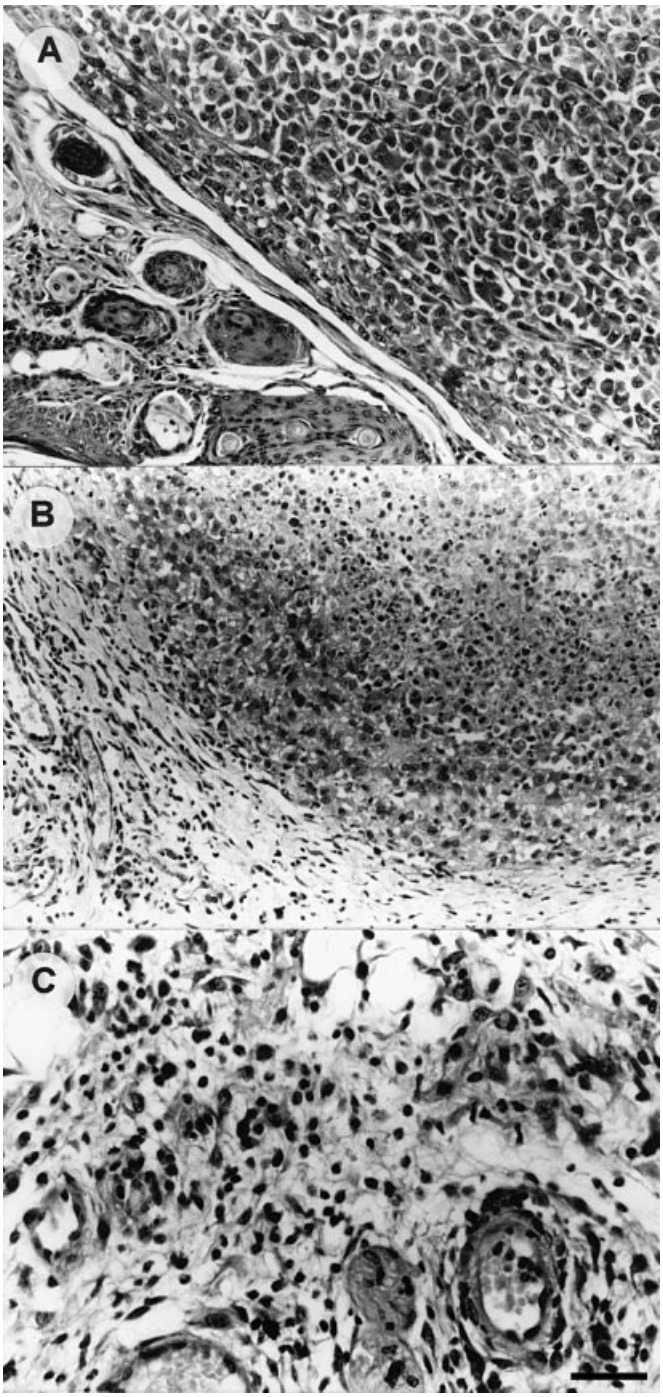

Figure 3. Tumor histologic examination. Hematoxylin–eosin staining of representative mice killed at day 3. (*A*) Tumor from group I with well-defined peritumoral and tumor areas. (*B*) Representative tumor from group II with extensive intratumoral necrotic area and fibrous surrounding tissue with an important leukocyte infiltration. (*C*) Tumor from group IV showing a high density of vessels and inflammatory infiltrate around them. *Scale bar*: (*A*, *B*) 5 μm; (*C*) 2.5 μm.

Our preliminary results on GM-CSF addition to cryosurgically treated tumors are promising, as an early intratumoral arrival of inflammatory cells would be favored. The immunostimulatory effect of this cytokine is being increasingly characterized, with evidence stemming from clinical and experimental approaches. Comparison between these approaches is extremely difficult, however; for instance, with respect to intratumoral injection of GM-CSF (Si *et al*, 1996; Nasi *et al*, 1999), the intratumoral doses administered in clinical trials (i.e., 10–80 μg per injection per tumor site; Nasi *et al*, 1999) could hardly be attained in murine models for tumors of similar size due to several orders of magnitude difference in total weight and the probable ensuing toxicity.

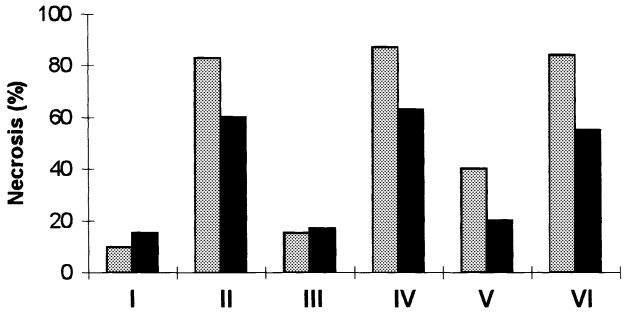

Figure 4. Image analysis of tumor necrosis. Quantitations were performed with an image analyzer in samples at day 3 (light bars) and day 15 (dark bars). One representative experiment of three is shown. Treatments applied to groups I–VI are described in **Table II**.

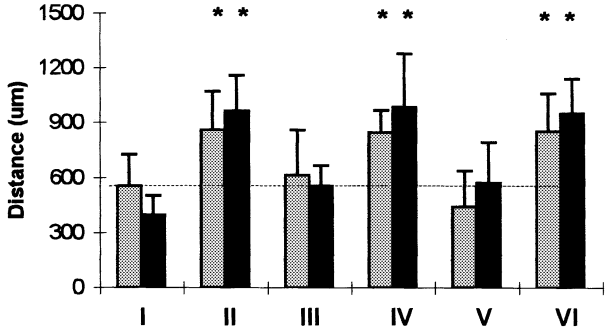

Figure 5. Image analysis of peritumoral edema. Distances (in μm) between epidermis and tumor were measured at day 3 (light bars) and day 15 (dark bars). The horizontal dotted line indicates the distance in nontreated animals. Above this line, the existence of edema is assumed. Measurements were performed at original magnification, × 25 in 10 fields per sample. Treatments groups are described in **Table II**. *$p < 0.01$.

Finally, the observation that an antibody response was triggered in cryosurgically treated mice, but not in untreated mice is highly relevant, as antibodies may play a part in anti-tumoral defense through complement activation or antibody-dependent cell-mediated cytotoxicity. In our experimental setting, antibody response is probably T cell independent. Nonetheless, some nude mice preserve a small rudimentary cystic thymus (Hsu *et al*, 1975), which could account for the low levels of IgG2a antibodies occasionally found (data not shown). It should be taken into account, however, that the switch IgM–IgG3 is T cell independent (Mongini *et al*, 1982).

The antibody response observed in this xenograft model is predictably directed against normal human antigens, probably as well as against tumor antigens because both would be seen as ''non-self'' molecules by the nude mice. The presence of specific antibodies targeting tumor cells and a dense granulocyte infiltration would contribute to tumor cell death. Local antibody-dependent cell-mediated cytotoxicity could be potentiated in the presence of GM-CSF by priming granulocytes for greater cytotoxicity (Kushner and Cheung, 1989).

The results obtained in this study suggest that this model may provide a clearer picture of the mechanisms that could be used to increase intratumoral leukocyte infiltration, and these studies should be pursued and extended to immunocompetent models for a full comprehensive analysis.

This work was supported by grants from the following Institutions: CONICET, University of Buenos Aires, Agencia para el Desarrollo Científico y Tecnológico, Fundación Sales, Fundación para la Investigación y Prevención del Cáncer (FUCA), Fundación Mosoteguy, and Fundación María Calderón de la Barca, Argentina. JM and RW are Career Investigators from CONICET; SG is a Fellow from the CONICET; SRG is a Fellow from the University of Buenos Aires and AB is a Fellow from Fundación Sales. The technical assistance of F. Fraga and E. Roger in animal care is gratefully acknowledged.

Table III. Inflammatory cells quantitation[a]

	Peritumoral				Intratumoral			
	PMN[b]		M[b]		PMN[b]		M[b]	
Groups	Day 3	Day 15	Day 3	Day 15	Day 3	Day 15	Day 3	Day 15
I	0 (0–5)	0 (0–5)	1 (0–9)	0 (0–3)	0 (0–1)	0 (0–5)	0 (0–2)	0 (0–3)
II	20[c] (2–150)	1[c] (0–20)	12[c] (3–150)	9[c] (0–28)	0 (0–12)	0 (0–4)	0 (0–2)	0 (0–3)
III	0 (0–8)	0 (0–16)	3[c] (0–19)	0 (0–9)	0 (0–1)	0 (0–5)	1 (0–6)	0 (0–2)
IV	20[c] (2–150)	1 (0–58)	13[c] (3–100)	4[c] (0–30)	2[cd] (0–34)	1[c] (0–14)	2[cd] (0–37)	2[c] (0–11)
V	0 (0–4)	0 (0–3)	0 (0–2)	0 (0–3)	0 (0–2)	0 (0–4)	0 (0–1)	0 (0–5)
VI	20[c] (2–150)	1[c] (0–15)	12[c] (0–150)	5[c] (0–28)	0 (0–10)	0 (0–4)	0 (0–2)	0 (0–3)

[a]Values (cells per HPF) are expressed as medians. Ranks are shown in brackets.
[b]Polymorphonuclear leukocytes (PMN) and macrophages (M) were evaluated in at least 10 fields per mice.
[c]($p = 0.01$); compared with untreated group (Wilcoxon test).
[d]($p = 0.01$); compared with cryotreated group (Wilcoxon test).

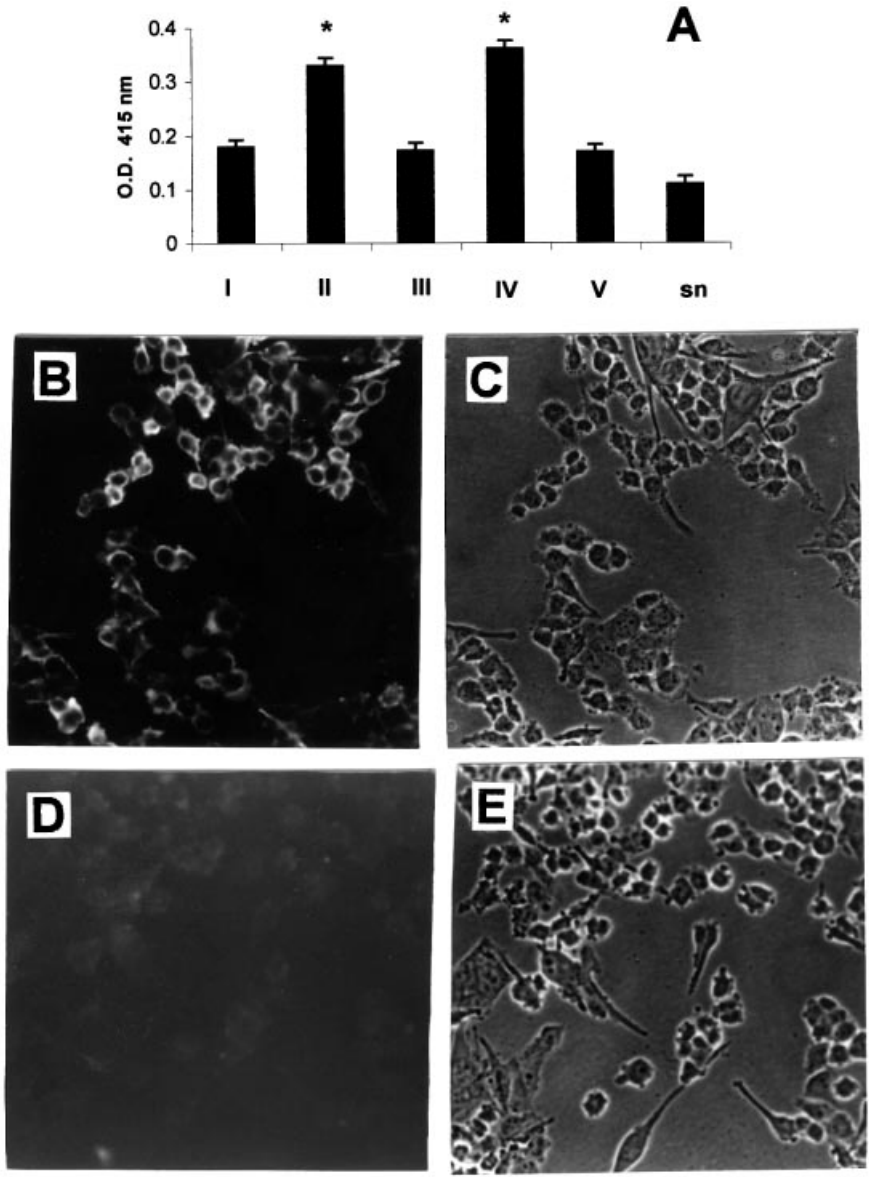

Figure 6. Antibody generation by cryosurgery treatment. (a) Immunoreactivity of sera evaluated by enzyme-linked immunosorbent assay. Values for groups I, III, and V correspond to eight to 10 animals. For groups II and IV, only positive sera (four of 10 mice for each group) are represented. Sera from group VI were not tested for reactivity. Normal mice serum was also assayed (sn). *$p < 0.004$, as compared with groups I, III, and V. (b) Representative immunofluorescence with reactive sera from groups II and IV was performed as described under *Materials and Methods*. (*c*) Phase contrast image corresponding to *b*. (d) Representative immunofluorescence with sera from group I. (*e*) Phase contrast image corresponding to *d*. *Scale bar*: 11.11 μm.

Table IV. Analysis of specificity of mice reactive sera[a]

Cell type	Cell line	PBS	Group I sera	Group II sera	Group IV sera
Human melanoma	IIB-MEL-J	–	+	+++	+++
Human melanoma	IIB-MEL-IAN	–	±	+++	+++
Human melanoma	IIB-MEL-LES	–	+	+++	++
Human breast adenocarcinoma	MCF-7	–	+	+++	++
Human peripheral blood mononuclear cells		–	±	+/++ (Ly)[b] – (Mo)[b]	+/++ (Ly)[b] – (Mo)[b]
Murine melanoma	Bl6-F1	–	+	+	+
Murine microvascular endothelial cells	1G11	–	±	±	±

[a]Data correspond to semiquantitative evaluations performed in immunofluorescence assays using mycoplasma-free cell lines. Three independent experiments were done.
[b]Freshly isolated lymphocytes (Ly) and monocytes (Mo) from a healthy donor were used as normal human cell control.

REFERENCES

Ballaré C, Barrio M, Portela P, Mordoh J: Functional properties of FC-2.15, a monoclonal antibody that mediates human complement cytotoxicity against breast cancer cells. *Cancer Immunol Immunother* 41:15–22, 1995

Bennett SR, Carbone FR, Karamalis F, Miller JF, Heath WR: Induction of a CD8+ cytotoxic T lymphocyte response by cross-priming requires cognate CD4+ T cell help. *J Exp Med* 186:65–70, 1997

Burgess A, Camakaris J, Metcalf D: Purification and properties of colony-stimulating factor from mouse lung-conditioned medium. *J Biol Chem* 252:1998–2003, 1977

Capurro M, Bover L, Portela P, Livingston P, Mordoh J: FC-2.15, a monoclonal antibody active against human breast cancer, specifically recognizes Lewis^x hapten. *Cancer Immunol Immunother* 45:334–339, 1998

Clynes R, Takechi Y, Moroi Y, Houghton A, Ravetch JV: Fc receptors are required in passive and active immunity to melanoma. *Proc Natl Acad Sci USA* 95:652–656, 1998

Cotran RS, Pober JS: Endothelial activation. Its role in inflammatory and immune reactions. In: Simionescu N, Simionescu M (eds). *Endothelial Cell Biology*. New York: Plenum, 1988, pp 335–347

Dong QG, Bernasconi S, Lostaglio S, *et al*: A general strategy for isolation of endothelial cells from murine tissues. *Arterioscler Thromb Vasc Biol* 17: 1997

Dranoff G, Jaffee A, Lazenby P, *et al*: Vaccination with irradiated tumor cells engineered to secrete human granulocyte-macrophage colony-stimulating factor stimulates potent, specific and long-lasting antitumor immunity. *Proc Natl Acad Sci USA* 90:3539, 1993

Gallucci S, Lolkema M, Matzinger P: Natural adjuvants: endogenous activator of dendritic cells. *Nat Med* 5:1249–1255, 1999

Guerra L, Mordoh J, Slavtsusky Y, Larripa Y, Medrano E: Characterization of IIB-Mel J. A new and highly heterogeneous human melanoma cell line. *Pigment Cell Res* 2:504–509, 1989

Hernberg M, Turunen J, Muhonen T, Pyrhönen S: Tumor infiltrating lymphocytes in patients with metastatic melanoma receiving chemoimmunotherapy. *J Immunother* 20:488–495, 1997

Hsu CK, Whitney RA, Hansen CT: Thymus-like lymph node in nude mice. *Nature* 257:681–682, 1975

Huang AY, Golumbek P, Ahmadzadeh M, Jaffee E, Pardoll D, Levitsky H: Role of bone marrow-derived cells in presenting MHC class I-restricted tumor antigens. *Science* 264:961–965, 1994

Kairiyama C, Slavutsky I, Larripa I, et al: Biologic immunocytochemical, and cytogenetic characterization of two new human melanoma cell lines: IIB-MEL-LES and IIB-MEL-IAN. *Pigment Cell Res* 8:121–131, 1995

Kimber I, Cumberbatch M, Dearman RJ, Bhushan M, Griffiths CE: Cytokines and chemokines in the initiation and regulation of epidermal Langerhans cell mobilization. *Br J Dermatol* 142:401–412, 2000

Klein C, Bueler H, Mulligan RC: Comparative analysis of genetically modified dendritic cells and tumor cells as therapeutic cancer vaccines. *J Exp Med* 191:1699–1708, 2000

Kushner BH, Cheung NK: GM-CSF enhances 3F8 monoclonal antibody-dependent cellular cytotoxicity against human melanoma and neuroblastoma. *Blood* 73:1936–1941, 1989

Mazur P: Freezing of living cells: Mechanisms and implications. *Am J Physiol* 247:125–142, 1984

Mongini PK, Paul WE, Metcalf ES: T cell regulation of immunoglobulin class expression in the antibody response to trinitrophenyl-ficoll. Evidence for T cell enhancement of the immunoglobulin class switch. *J Exp Med* 155:884–902, 1982

Morvillo V, Bover L, Mordoh J: Identification and characterization of 14 kDa immunosuppressive protein derived from IIB-MEL-L, a human melanoma cell line. *Cell Mol Biol* 42:779–795, 1996

Nasi ML, Lieberman P, Busam KJ, *et al*: Intradermal injections of granulocyte-macrophage colony-stimulating factor (GM-CSF) in patients with metastatic melanoma recruits dendritic cells. *Cytokines Cell Mol Ther* 5:139–144, 1999

Nooijen P, Eggermont A, Schalkwijk L, Henzen-Logmans S, de Waal R, Ruiter D: Complete response of melanoma-in-transit metastasis after isolated limb perfusion with tumor necrosis factor alpha and melphalan without massive tumor necrosis: a clinical and histopathological study of the delayed-type reaction pattern. *Cancer Res* 58:4880–4887, 1998

Orpwood RD: Biophysical and engineering aspects of cryosurgery. *Phys Med Biol* 26:555–575, 1981

Randolph GJ, Inaba K, Robbiani DF, Steinman RM, Muller WA: Differentiation of phagocytic monocytes into lymph node dendritic cells in vivo. *Immunity* 11:753–761, 1999

Sauter B, Alberta M, Franciscoa L, Larssona M, Somersana S, Bhardwaj N: Consequences of cell death: exposure to necrotic tumor cells, but not primary tissue cells or apoptotic cells, induces the maturation of immunostimulatory dendritic cells. *J Exp Med* 191:423–434, 2000

Shutt DC, Daniels KJ, Carolan EJ, Hill AC, Soll DR: Changes in the motility, morphology and F-actin architecture of human dendritic cells in an in vitro model of dendritic cell development. *Cell Motil Cytoskeleton* 46:200–221, 2000

Si Z, Hersey P, Coates AS: Clinical responses and lymphoid infiltrates in metastatic melanoma following treatment with intralesional GM-CSF. *Melanoma Res* 6:247–255, 1996

Soiffer R, Lynch M, Mihm M, *et al*: Vaccination with irradiated autologous melanoma cells engineered to secrete human granulocyte-macrophage colony-stimulating factor generates potent antitumor immunity in patients with metastatic melanoma. *Proc Natl Acad Sci USA* 95:13141, 1998

Soule HD, Vazquez J, Long A, Albert S, Brennan M: A human cell line from a pleural effusion derived from a breast carcinoma. *J Natl Cancer Inst* 51:1409–1415, 1973

Springer TA: Traffic signals for lymphocyte recirculation and leukocyte emigration: the multistep paradigm. *Cell* 76:301–314, 1994

Szabolcs P, Avigan D, Gezelter S, Ciocon DH, Moore MA, Steinman RM, Young JW: Dendritic cells and macrophages can mature independently form a human bone marrow-derived, post-colony-forming unit intermediate. *Blood* 87:4520–4530, 1996

Turk T, Rees M, Pietrow P, Myers C, Mills C, Gillenwater J: Determination of optimal freezing parameters of human prostate cancer in a nude mice model. *Prostate* 38:137–143, 1999

Wells A, Malkovsky M: Heat shock proteins, tumor immunogenicity and antigen presentation: an integrated review. *Immunol Today* 21:129–132, 2000

Wing EJ, Magee DM, Whiteside TL, Kalan SS, Shadduck RK: Recombinant human granulocyte/macrophage colony-stimulating factor enhances monocyte cytotoxicity and secretion of tumor necrosis factor alpha and interferon in cancer patients. *Blood* 73:643–646, 1989

Zouboulis ChC: Principles of cutaneous cryosurgery. An update. *Dermatology* 198:111–117, 1999